Thermal Science and Engineering (2021) Volume 4 Issue 2
doi:10.24294/tse.v4i2.1520

ORIGINAL RESEARCH ARTICLE

Study on combustion characteristics of swirl premixed combustor

Zhihao Zhang, Xiao Liu*, Tiezheng Zhao, Gang Liu, Guangpu Lv, Hongtao Zheng

College of Power and Energy Engineering, Harbin Engineering University, Harbin 150001, China. E-mail: Liuxiao_heu@163.com

ABSTRACT

Taking a certain type of combustion chamber as the research object, the numerical simulation is carried out by using RANS (Reynolds averaged Navier-stokes) and LES (large eddy simulation), and the simulation results of the two numerical methods are compared and analyzed. The research results show that the RANS calculation results can reflect the main flow field characteristics in the combustion field, and have certain engineering significance. LES can reproduce specific flow field details such as the weak axial flow region, accurately simulate the location and strength of the shear layer, simulate the dynamic development process of flame, and capture the dynamic characteristics of the combustion flow field. Compared with RANS, LES has more obvious advantages in numerical simulation of the combustion flow field. Through calculation, the precessing vortex core under this working condition is composed of three relatively independent spiral vortex branches, which excites periodic velocity pulsation and pressure pulsation in the combustion chamber. LES captures the dominant frequency with the precession vortex core of 156 Hz.

Keywords: Swirl Premixed Combustion Chamber; Partial Premixed Combustion; Large Eddy Simulation; Precessing Vortex Core

ARTICLE INFO

Received: 12 September 2021
Accepted: 1 November 2021
Available online: 13 November 2021

1. Introduction

With the increasingly prominent problem of environmental pollution and the increasing awareness of environmental protection around the world, international organizations have Formulated strict air pollutant emission standards for combustion systems, requiring gas turbines and aero-engines to continuously reduce pollutant emission levels. Therefore, low pollutant emission technology has become one of the key technologies with great development prospects. When designing and developing a new generation of gas turbines, manufacturers often adopt lean premixed combustion technology to replace the traditional diffusion combustion[1,2]. The characteristic of lean burn premixed combustion technology is that the fuel and oxidant have been fully mixed before entering the combustion chamber. By controlling the mixing ratio of fuel and oxidant, the flame temperature can be reduced to achieve the purpose of reducing pollutant emissions. However, lean premixed combustion is close to the lean flameout boundary, which is prone to combustion instability[3], so the swirl generated by the cyclone is needed to stabilize the flame. As a typical representative of an advanced combustion chamber, the combustion characteristics of swirl premixed combustion chambers have attracted extensive attention of experts and scholars all over the world.

With the continuous improvement of computer ability, computational fluid dynamics (CFD) has become an indispensable means in practical engineering design and application, playing a huge role. Aiming at the complex physical and chemical process of swirl and combustion coupling in an advanced combustion chamber, the coupling analysis method of turbulence model and combustion model in CFD method can effectively analyze this complex process. Turbulence numerical simulation methods are mainly divided into three categories: direct numerical simulation method (DNS), Reynolds average (RANS) statistical method, and large eddy simulation (LES) method. Limited by the amount of calculation, DNS is mainly applied to the theoretical research of low Reynolds numbers at this stage. RANS method has been widely used in engineering because of its small amount of calculation, but because its calculation results have no time correlation, it cannot capture the dynamic information of a swirling combustion field. LES method is between the two. It uses a low-pass filter function to filter small-scale turbulent motion and directly solve unsteady large-scale vortex motion. It can reproduce the real process of swirl combustion to a certain extent and has broad application prospects.

Wang[4] took the round hole jet as the model and compared the calculation results of DNS, LES, and RANS models for turbulence. The research showed that RANS simulated the first-order statistics (such as the length of the recirculation core) more accurately, but the prediction accuracy of the peak value of the second-order stress was poor. DNS could provide model correction for LES and RANS. He *et al*.[5] used RANS coupling different combustion models to conduct numerical analysis of gas turbine combustion. Yang and Zheng[6] used the RANS model to conduct numerical research on the combustion process of the chemical regenerative cycle combustion chamber, and the calculation results have certain engineering significance.

Balut *et al*.[7] successfully applied LES to the numerical study of industrial gas turbines. The experimental study shows that LES can not only well reproduce the details of the combustion flow field, but also accurately calculate a variety of intermediates in the combustion process, pointing out the direction for the dynamic simulation of the combustion process. Han *et al*.[8] used the LES method to simulate stratified swirl flame, and successfully captured the details of combustion flow field such as vortex breaking and central recirculation zone.

Most studies at home and abroad simply described that the LES numerical method is more accurate than the RANS numerical method, and did not compare the calculation results of the two models in detail. Taking the combustion chamber of an industrial gas turbine as a model for numerical analysis, this paper compares and discusses in detail the simulation of the swirl combustion chamber by RANS and LES, analyzes the reproduction ability of the two numerical simulation methods on the swirl combustion information, summarizes the application scope of the two models, and deeply analyzes the LES numerical results to obtain the transient structure of the combustion flow field and the pressure pulsation information. This method can be used in the later numerical research of the combustion chamber.

2. Mathematical model

In this paper, k-ε model and LES-WMLES model are coupled with the FGM combustion model to simulate the swirling combustion process.

2.1 Realizable k-ε model

Compared with the standard k-ε model, the realizable k-ε model improves the calculation Formula and ε equation of turbulent viscosity, which is suitable for simulating the flow problems such as strong streamline bending, vortex and rotation。 Therefore, the realizable k-ε model turbulence model is applied in the RANS simulation of the combustion chamber in this paper.

The realizable k-ε equation of the model is

$$\frac{\partial(\rho k u_j)}{\partial x_j} = \frac{\partial}{\partial x_j}\left[\left(\mu + \frac{\mu_t}{\sigma_k}\right)\frac{\partial k}{\partial x_j}\right] - \rho\epsilon + S_k \tag{1}$$

$$\frac{\partial(\rho\varepsilon u_j)}{\partial x_j} = \frac{\partial}{\partial x_j}\left[\left(\mu + \frac{\mu_t}{\sigma_\varepsilon}\right)\frac{\partial\varepsilon}{\partial x_j}\right] - \rho C_1 S_\varepsilon - \rho C_2 \frac{\varepsilon^2}{k + \sqrt{v\varepsilon}} + C_{1\varepsilon}\frac{\varepsilon}{k}C_{3\varepsilon}G_b + S_\varepsilon \quad (2)$$

Where: $\sigma_k = 1.0$, $\sigma_\varepsilon = 1.2$, $C_2 = 1.9$, $C_1 = max\left(0.43, \frac{\eta}{\eta+5}\right)$, $\eta = S\frac{k}{\varepsilon}$, $S = \sqrt{2S_{ij}S_{ij}}$.

Where: ρ is the density, kg/m^3; k is turbulent kinetic energy, W/(m·K); ε is turbulent dissipation rate; u_i, u_j are speed, m/s; x_i, x_j are the unit length in each direction; S_k is the source item; μ_t is turbulent viscosity, (N·s)/m^2.

2.2 LES model

Compared with RANS model, LES can capture flow field information more accurately. LES directly solves the large-scale turbulence, and uses the sub-grid model to solve the remaining small-scale turbulence. The filtered N-S equation can be expressed as

$$\frac{\partial\bar{\rho}}{\partial t} + \frac{\partial\bar{\rho}\tilde{u}_i}{\partial x_i} = 0 \quad (3)$$

$$\frac{\partial\bar{\rho}\tilde{u}_i}{\partial t} + \frac{\partial(\bar{\rho}\tilde{u}_i\tilde{u}_j)}{\partial x_j} = -\frac{\partial\sigma_{ij}}{\partial x_j} - \frac{\partial\bar{p}}{\partial x_i} + \frac{\partial_{ij}^{sgs}}{\partial x_j} \quad (4)$$

$$\frac{\partial\bar{\rho}\widetilde{Y_K}}{\partial t} + \frac{\partial(\bar{\rho}\widetilde{Y_K}\tilde{u}_j)}{\partial x_j} = \frac{\partial}{\partial x_j}\left(\bar{\rho}\widetilde{D_k}\frac{\partial\widetilde{Y_k}}{\partial x_j}\right) - \frac{\partial}{\partial x_j}\left(\bar{\rho}\widetilde{u_j Y_k} - \bar{\rho}\tilde{u}_j\widetilde{Y_k}\right) + \overline{\omega_k}, k = 1, \dots, N \quad (5)$$

$$\frac{\partial\bar{\rho}\tilde{h}}{\partial t} + \frac{\partial(\bar{\rho}\tilde{u}_j\tilde{h})}{\partial x_j} = \frac{D\bar{p}}{Dt} - \frac{\partial}{\partial x_j}\left(\bar{\rho}\widetilde{u_j h} - \bar{\rho}\tilde{u}_j\tilde{h}\right) + \frac{\partial}{\partial x_j}\left(\overline{\rho a}\frac{\partial\tilde{h}}{\partial x_j}\right) + \overline{\tau_{ij}\frac{\partial u_i}{\partial x_j}} \quad (6)$$

In LES model, Bossinesq hypothesis τ_{ij}^{sgs} is used to describe:

$$\tau_{ij}^{sgs} = \bar{\rho}\left(\widetilde{u_i u_j} - \tilde{u}_i\tilde{u}_j\right) = -2\mu_{sgs}\widetilde{S_{ij}^D} + \frac{2}{3}\bar{\rho}k\delta_{ij} \quad (7)$$

The algebraic wall modeled LES model (WMLES) uses the Reynolds average method to simulate the convection field in the boundary layer, while the large eddy simulation method is used outside the near wall region, and its eddy viscosity is defined as

$$\mu_t = \min\left[(\kappa d_w)^2, (C_{Smag}\Delta)^2\right] \cdot S\left\{1 - e^{[-(y^+/25)^3]}\right\} \quad (8)$$

Where: d_w is the distance between the point and the wall, S is the strain rate, parameter κ = 0.41, C_{smag} = 0.2 and filter size Δ is selected according to specific flow field conditions:

$$\Delta = min\left(max(C_w \cdot d_w \cdot C_w \cdot h_{max}; h_{wn}\right); h_{max} \quad (9)$$

Where: h_{wn} is the grid step along the normal direction of the wall, h_{max} is the maximum step of the wall grid, and C_w is taken as the fixed value of 0.15.2.3 FGM (flamelet generated manifold) model

The FGM model refers to the laminar flame surface method, and considers that the three-dimensional flame has a one-dimensional structure in essence, and the turbulent flame surface is the statistical average of the laminar flame surface, so the one-dimensional flame can be used to construct the reaction mechanism subspace. FGM model can consider the influence of convection and diffusion, and it has good accuracy in both high-temperature and low-temperature regions. In addition, FGM can also be naturally extended from premixed combustion model to partial premixed combustion model, rather than rough and simple combination[9], so its applicability is wider and closer to reality. FGM partial premixed combustion model is adopted in this paper.

In order to use FGM method to simulate the combustion flow field, it is necessary to use chemical reaction mechanism to establish laminar small flame form. In this paper, GRI 3.0 mechanism (detailed chemical reaction mechanism of methane) is used; the mixed score can be defined as[10]:

$$Z = \frac{Z_i - Z_{i,ox}}{Z_{i,fuel} - Z_{i,ox}} \quad (10)$$

Where: Z_i is the relative atomic mass of component *i*, and the subscripts OX and fuel represent oxidant and fuel, respectively. The mixing fraction is a conservative scalar, which is only affected by diffusion and convection. Its transport equation is

$$\frac{\partial}{\partial t}(\rho Z)+\frac{\partial}{\partial_{xi}}(\rho u_i Z)=\frac{\partial}{\partial_{xi}}(\rho D\frac{\partial Z}{\partial_{xi}}) \tag{11}$$

Where, *D* is the laminar diffusion coefficient.

The selection of reaction progress variable *C* is defined based on components, as shown in Formula (12):

$$C=\frac{\sum_k \alpha_k (Y_k - Y_k^u)}{\sum_k \alpha_k (Y_k^{eq} - Y_k^u)}=\frac{Y_C}{Y_C^{eq}} \tag{12}$$

3. Physical model and boundary conditions

3.1 Introduction to a model combustion chamber

The central section of a model combustion chamber is shown in **Figure 1**. In order to facilitate the installation and testing of test equipment, the model combustion chamber simplifies the flame tube of the prototype combustion chamber[11]. The length and width of the cross section of the combustion chamber are 0.165 m, and the length of the transition section is 0.188 m. The radial hydro cyclone is installed at the head of the combustion chamber and is composed of 12 fixed wedges with a swirl number of 1.3. The premixed fuel nozzle is located in the rectangular channel near the inlet of the hydro cyclone. The fuel is injected into the inter blade channel to mix with the incoming air, and then flows into the combustion chamber for combustion after passing through the premixed section.

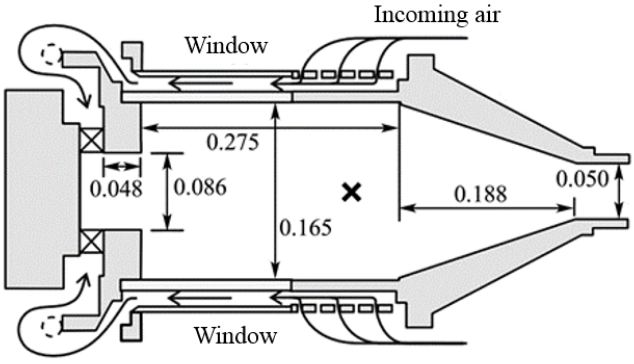

Figure 1. Combustor[11] (unit: m).

3.2 Grid division

As shown in **Figure 2**, the CFD pre-processing software ICEM is used to divide the global structured grid of the calculation domain, which includes the radial hydro cyclone, the premixed section, the model combustion chamber and the outlet of the transition section. The hydro cyclone and the shear layer area are meshed to increase the simulation accuracy, and the rougher mesh is used in the outlet area of the combustion chamber to improve the calculation efficiency. In this paper, the same set of grids is used to simulate RANS and LES, and the results of the two turbulence simulation methods are compared. The specific parameters of the grid are shown in **Table 1**:

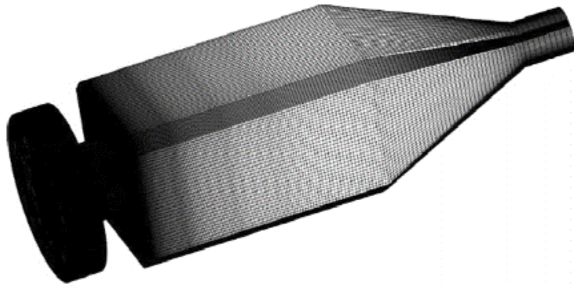

Figure 2. Grid of combustor calculation domain.

Table 1. Grid parameters

Grid quantity/pc	Δx_{min}/mm	Δx_{max}/mm	Δy_{min}/mm	Δy_{max}/mm	Δz_{min}/mm	Δz_{max}/mm
7,315,859	0.053	4.340	0.053	4.340	0.125	6.210

3.3 Boundary conditions

The inlet section of air and fuel is defined as the mass flow inlet, and the test fuel is German natural gas[11] The fuel composition is shown in **Table 2**. Inlet air pressure p = 0.3 MPa, air mass flow 175.0 g/s, fuel mass flow 6.2 g/s. The air temperature is 685.0 K and the fuel temperature is 319.8 K. The outlet adopts the boundary condition of pressure outlet, and the pressure loss is 1%.

Table 2. Components in German natural gas

Component	Mole fraction/%
CH_4	96.970
C_2H_6	1.553
C_3H_8	0.400
CO_2	0.270
N_2	0.753

4. Result analysis

4.1 Comparison of numerical simulation results between LES and RANS

Stopper *et al*.[11] monitored the speed, temperature and mixed scores etc. of the four positions. The distances between different straight lines and the duty plane are 1.21 *D*, 1.44 *D*, 1.66 *D* and 2.00 *D*, respectively, and *D* is the diameter of the premixed section. **Figures 3** and **4** show the numerical results of RANS and the comparison of LES time average velocity and temperature distribution with experimental data.

It can be seen from **Figure 3** that the calculated results better reflect the time average axial velocity distribution in the combustion chamber, and the calculated value of the velocity peak u_{max} is close to the experimental value. There is a big difference between the axial velocity test value and the numerical simulation result at position 3, and the calculation error is about 5%. The center and corner vortex recirculation region in the combustion flow field are accurately reproduced. There is a symmetrical central recirculation zone in the center of the combustion chamber, and the width of the central recirculation zone obtained by simulation is slightly wider than that of the test. The calculation error of RANS in the width of the recirculation zone is about 7%, and the calculation error of LES is small, about 2%. Due to the high swirl intensity, a local negative velocity zone appears near the central axis. This strong swirl in the combustion field will cause a large number of high-temperature burned products to reflux, and preheat and ignite the premixed gas upstream of the combustion chamber.

It can be clearly seen from **Figure 3** that, compared with RANS, LES is in good agreement with the experimental data, which can well reflect the details of the velocity field, well predict the range and strength of the shear layer, and also capture the weak central recirculation zone near the central axis downstream of the combustion field, which is consistent with the results of the boundary limited swirl test observed in the early test[12]. However, RANS can only roughly describe the shape of the central recirculation zone and the angular vortex recirculation zone, the distribution law and development trend of rough reaction speed, temperature and other parameters, and cannot accurately reproduce the internal details and recirculation characteristics of the central recirculation zone, which will have a great impact on the prediction of the combustion field and the distribution of components in the combustion chamber, especially the time independent calculation method of RANS cannot reflect the details of the combustion dynamic process. The dynamic process of flame stability and ignition flameout cannot be captured, and the degree of application is limited.

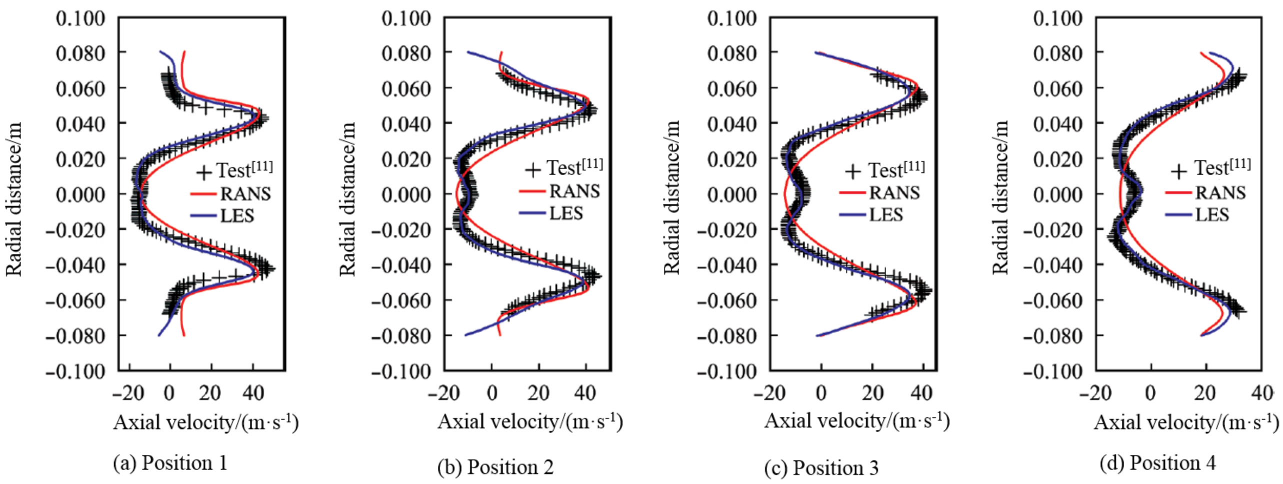

Figure 3. Axial velocity indifferent positions.

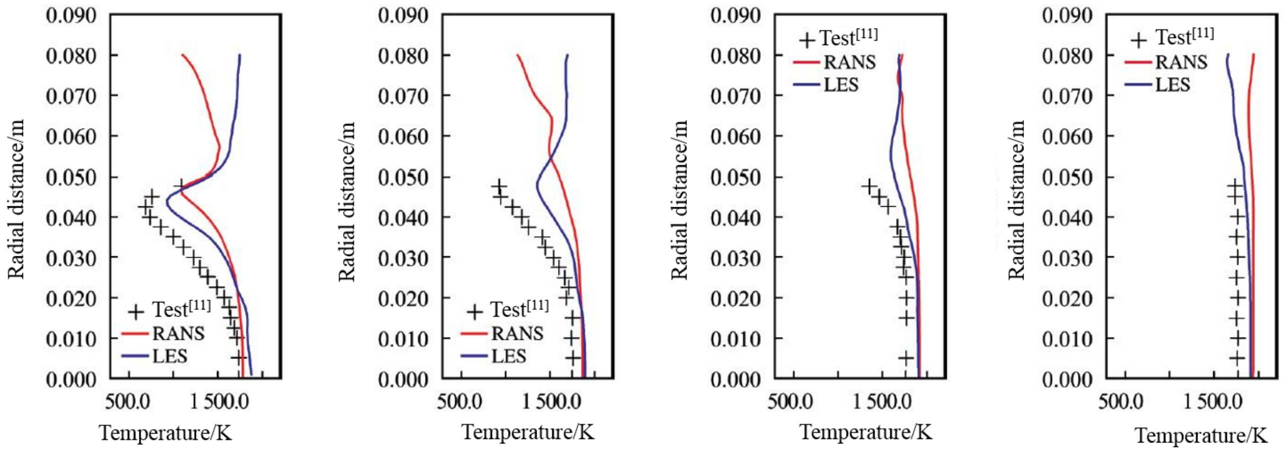

(a) Position 1 (b) Position 2 (c) Position 3 (d) Position 4

Figure 4. Temperature indifferent positions.

4.2 Reproduction of flow field details

Figure 5 shows the instantaneous combustor head velocity, mixing fraction and temperature simulated by LES. The air carries the fuel injected into the inter blade passage through the cyclone into the combustion chamber, and forms a shear layer along the wall of the premixed chamber. As shown in **Figure 5(b)**, the vortex generated by the strong momentum exchange in the shear layer carries the fuel downstream of the combustion chamber. The fuel and air are strongly mixed in the shear layer to form a premixed gas and flow downstream. When the premixed gas meets the high-temperature products entrained back downstream, it begins to burn rapidly. The recirculation effect of strong swirling flow and strong velocity pulsation in the shear layer stabilize the flame position near the shear layer. From the mixture fraction distribution diagram and temperature cloud diagram, it can be seen that the combustion mainly occurs at the position where the equivalence ratio is less than 1 (the mixture fraction is less than 0.055), and the combustion chamber is mainly in lean combustion state.

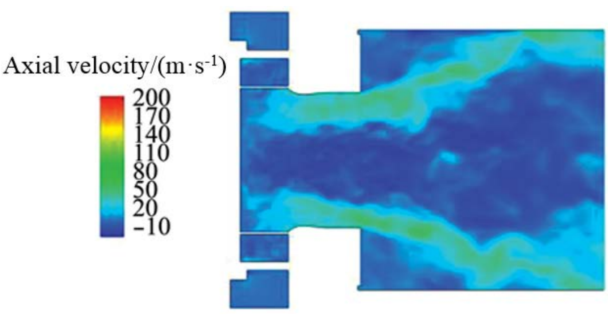

(a) Axial velocity

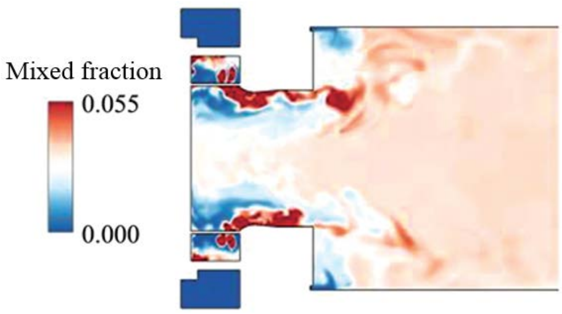

(b) Mixed fraction

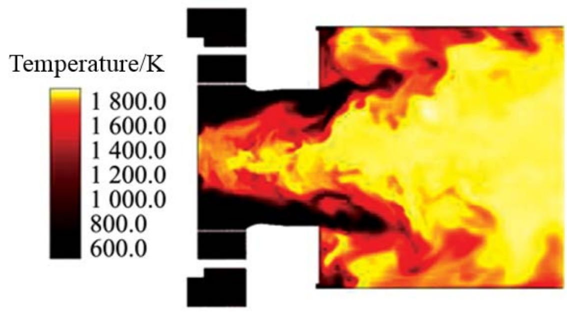

(c) Temperature

Figure 5. Contour of axial velocity mean mixture fraction and temperature in the combustor.

High swirling flow is often accompanied by the formation of precession vortex core. The vortex moves periodically around the central axis, which will cause velocity and pressure pulsation in the combustion chamber, affect the combustion process, and easily cause combustion oscillation, which will not only increase the emission of pollutants in the combustion process, but also have an adverse impact on the combustion equipment.

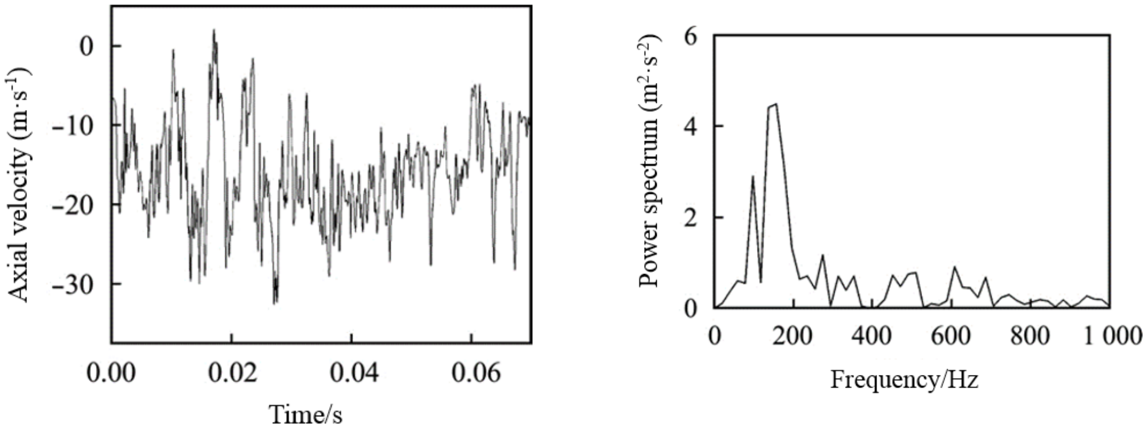

(a) Axial velocity time series distribution (b) Axial velocity power spectral density

Figure 6. Axial velocity at the inner shear layer.

LES simulates the premixed combustion flow field instantaneously, and selects a point on the inner shear layer to monitor the change of its axial velocity with time. As shown in **Figure 6(a)**, the FFT transformation of the axial velocity time series distribution is carried out to obtain the axial velocity power spectral density. According to **Figure 6(b)**, the main frequency of the axial velocity fluctuation is 156 Hz, which is the frequency of the precession vortex core of a certain combustion chamber under this working condition. The axial velocity fluctuation in the combustion flow field is caused by the periodic falling off of the precession vortex core. The main difference between the precession vortex core and the spiral vortex is that the precession vortex core rotates around the central axis, the fluid around the vortex core rotates around its internal vortex axis, and the spiral vortex only makes a spiral motion around its own axis.

Figure 7 shows the spatial three-dimensional structure of the precession vortex core using the pressure contour method. The precession vortex core is composed of the core of the main spiral vortex and the branches of the spiral vortex. The main spiral vortex starts from the duty plane of the premixed combustion chamber and develops downstream. With the increase of distance, the main spiral vortex splits into several branches, that is, multiple relatively independent small spiral vortices, which rotate around the central axis to form a precession vortex core structure. As shown in **Figure 8**, there are three low-pressure areas in the throat of the combustion chamber, namely the three branches of the main spiral vortex. The vortex centers of the three places are all off-axis and located near the inner shear layer. These three independent small spiral vortices spiral along their respective central axes and rotate around the central axis of the combustion chamber, causing periodic pressure and velocity pulsations in the combustion flow field, making the velocity pulsation and mixing transportation process of the shear layer more intense. Therefore, the capture of precession vortex core is very important for the study of combustion characteristics of swirling combustion field, especially for the study of flame dynamic characteristics.

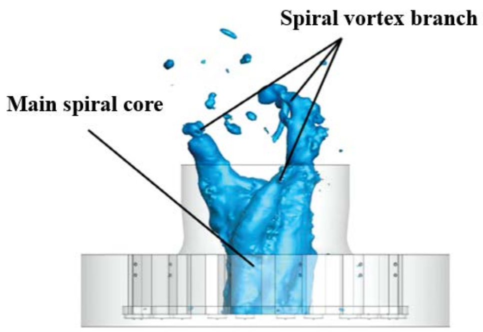

Figure 7. Precessing vortex core structure.

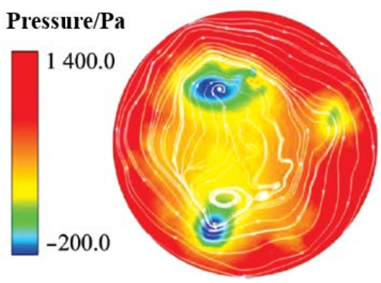

Figure 8. Pressure contour and streamlines of the combustor throat.

5. Conclusion

Based on CFD numerical simulation technology, this paper studies the numerical simulation of the combustion field of the swirl premixed combustion chamber. For a certain type of combustion chamber, the test results of the combustion chamber are reproduced by using the coupling calculation method of LES, RANS and FGM combustion model, respectively. The calculation results of the two numerical methods are compared, and the conclusion is obtained.

(1) The results of RANS can roughly describe the development trend of velocity field and temperature field, and can accurately calculate the size of velocity value, the location and strength of shear layer. It has certain engineering value.

(2) LES can accurately reproduce the detailed structure of the combustion flow field, and can capture the weak central recirculation zone at the axis of the restricted flow field. It is more accurate to calculate the range of shear layer. The dynamic calculation results of LES can capture the dynamic characteristics of combustion flow field, which is more in line with the needs of basic researchers.

(3) LES instantaneous numerical simulation can capture the precession vortex core in the strong swirl combustion flow field and analyze the dynamic characteristics of the flame. The numerical simulation shows that the dominant frequency of the precession vortex core is 156 Hz.

Acknowledgement

The National Science and Technology Major Special Fund Project (2017-III-0006-0031); the Central University Fundamental Research Fund Special Fund Project (3072019CFJ0307).

Conflict of interest

The authors declare that they have no conflict of interest.

References

1. Luciano E, Ballester J. Analysis of the dynamic response of premixed flames through chemiluminescence cross-correlation maps. Combustion and Flame 2018; 194: 296–308.
2. Patel N, Menon S. Simulation of spray–turbulence–flame interactions in a lean direct injection combustor. Combustion and Flame 2008; 153(1–2): 228–257.
3. El-Asrag HA, Iannetti AC, Apte SV. Large eddy simulations for radiation-spray coupling for a lean direct injector combustor. Combustion and Flame 2014; 161(2): 510–524.
4. Wang X. Investigation on the turbulance characteristics in the near field of round jet flow with DNS and RANS LES [MSc thesis]. Hangzhou: Zhejiang University; 2010.
5. He W, Zheng H, Cai L.Analysis of turbulent combustion model on numerical simulation of combustion chamber. Journal of Thermal Science and Technology 2011; 10(4): 360–365.
6. Yang H, Zheng H. Structural design and numerical simulation of dual-fuel gas turbine nozzle. Journal of Thermal Science and Technology 2010; 9(3): 78–85.
7. Bulat G, Jones WP, Marquis AJ. NO and CO formation in an industrial gas-turbine combustion chamber using LES with the Eulerian sub-grid PDF method. Combustion and Flame 2014; 161(7): 1804–1825.
8. Han X, Laera D, Morgans AS, *et al*. Flame macrostructures and thermoacoustic instabilities in stratified swirling flames. Proceedings of the Combustion Institute 2019; 37(4): 5377–5384.
9. Fluent Inc. Fluent user's guide.Canonsburg: PA: Ansys; 2017.
10. Bilger RW. Future progress in turbulent combustion research. Progress in Energy and Combustion Science 2000; 26(4–6): 367–380.
11. Stopper U, Meier W, Sadanandan R, *et al*. Experimental study of industrial gas turbine flames including quantification of pressure influence on flow field, fuel/air premixing and flame shape. Combustion and Flame 2013; 160(10): 2103–2118.
12. Syred N, Beer JM. Combustion in swirling flows: A review. Combustion and Flame 1974; 23(2): 143–201.